Modeling of Energy Savings Performed by a Barbecue Oven Isolated with Terracotta Bricks

Gaël Lassina Sawadogo[1*], Serge Wendsida Igo[2], Abdoulaye Compaore[2], Drissa Ouedraogo[1], David Namoano[1] and Joseph Dieudonne Bathiebo[1]

[1]*Université Joseph KI-ZERBO/Laboratoire d'Energies Thermiques Renouvelables (LETRE), Ouagadougou, Burkina Faso.*
[2]*Institut de Recherche en Sciences Appliquées et Technologies (IRSAT/CNRST), Département Energie, Ouagadougou, Burkina Faso.*

Authors' contributions

This work was carried out in collaboration among all authors. Author SWI designed the study, wrote the protocol and effect all necessary corrections. Author GLS performed the numerical simulations and wrote the first draft of the manuscript. Author JDB and AC managed the analyses of the study. Authors DO and DN managed the literature searches. All authors read and approved the final manuscript.

Original Research Article

ABSTRACT

This work is devoted to a numerical study of the energy savings achieved by an oven insulated with terracotta bricks compared to an uninsulated oven. The numerical methodology is based on the nodal method and the transfer equations were obtained by making an energy balance on each node. The equations were then discretized using an implicit scheme with finite differences and solved by the Gauss algorithm. Numerical results validated by the experiment show that the insulation of the oven with terracotta bricks considerably reduces the energy losses through the walls, but the reduction level varies according to the thickness of the bricks. The optimal thicknesses of the bricks are between 3 and 4 cm, which corresponds to energy savings of between 60 to 70% compared to the uninsulated oven. The energy saved increases the energy efficiency of the oven from 15-17% to 25-29%.

---

*Corresponding author: E-mail: bemagael@gmail.com;

ABBREVIATIONS

ε	:	*Emissivity of the wall*
λ	:	*Thermal conductivity* $(W.m^{-1}.K^{-1})$
ρ	:	*Density (kg.m^{-3})*
F	:	*Form factor*
v	:	*Kinematic viscosity of air (m^2.s^{-1})*
σ	:	*Stefan Boltzmann constant* $(5,67.10^{-8}m^{-2}K^{-4})$
μ	:	*Dynamic viscosity (Kg.m^{-1}.s^{-1})*
e	:	*Characteristic thickness (m)*
C_i	:	*Material heat capacity (kJ/kg.K)*
D	:	*Hydraulic diameter (m)*
F_{ciel}	:	*Sky form factor*
$g_{i,j}$	:	*Thermal conductance at nodes i and j (W.K^{-1})*
Gr	:	*Grashof number*
H	:	*Convection heat transfer coefficient* $(W.m^{-2}.K^{-1})$
h_r	:	*Radiative conductance* $(W.m^{-2}.K^{-1})$
h_a^e	:	*Enthalpy of air entering the node (J)*
h_a^s	:	*Enthalpy of air outing the node (J)*
m_i	:	*Mass of node i (Kg)*
$\dot{m}_{ai}^e$	:	*Mass air entering in the node i (Kg)*
$\dot{m}_{ai}^s$	:	*Mass air outing of the node i (Kg)*
Nu	:	*Nusselt number*
P	:	*Perimeter (m)*
Pr	:	*Prandlt number*
Re	:	*Reynolds number*
S	:	*Surface (m^2)*
$T_{i,j}$	:	*Temperature at nodes i and j (K)*
T_{ext}	:	*Ambient temperature (K)*
$T_{f-\text{int}}$	:	*Temperature of the internal face of the material (K)*
T_{f-ext}	:	*Temperature of the external face of the material (K)*
T_{sky}	:	*Sky temperature (K)*
V	:	*Air velocity (m/s)*
Qi	:	*Heat source at node i (J)*
λ_{char}	:	*Thermal conductivity of charcoal,*
e_{char}	:	*Charcoal thickness*
L	:	*Oven length (m)*
H	:	*Oven height (m)*
W	:	*Oven width (m)*
L_c	:	*Characteristic length (m)*

1. INTRODUCTION

In developing countries, biomass is the main source of energy used for cooking meals [1,2,3]. This situation has a negative impact on forest resources and several studies have raised the alarm about the regression of forest areas and its impact on the climate [4,5,6].

In recent years, with a view to control this problem, research has been directed towards the development of energy-efficient cooking technologies. The issue is also environmental because it is known that emissions from households cookstoves degrade air quality with harmful health and climatic consequences [7,8,9,10]. The environmental impact is greater in

the case of traditional cookstoves with a low energy efficiency [11]. Thus, from traditional 3-stone stoves, of which 85 to 90% of the energy is lost in the environment [12], improved stoves have been developed. Improvement technics vary from one stove to another, but most of them are based on insulating the wall of the stove. The insulation materials used are generally local (fired clay bricks, sun-dried bricks, clay, etc.). Several studies have shown that insulation materials have significantly improved the energy efficiency of cookstoves and reduced emissions compared to 3-stone cookstoves [13,14,15,16].

However, the improvements were mainly concentrated in the household cookstoves. In Burkina Faso, grillers continue to use uninsulated metal ovens with the same disadvantages as those associated with the use of traditional cookstoves. In addition, the lack of insulation exposes grillers to high temperatures and shortens the useful life of the equipment. In our previous work, we have shown that these equipment lost half of the energy consumed in the environment through the walls [17].

It is therefore important to insulate the walls of these ovens in order to correct their energy shortcomings. Among the insulating materials recommended for ovens are refractory materials, including terracotta bricks. These materials are able to withstand high temperatures and sudden temperature changes [18,19]. In addition, terracotta bricks have good thermophysical properties [20,21] and are produced locally.

However, before developing an isolated prototype with these materials, it is important to have simulated results on the thermal behavior of the new oven. This is why the aim of this work is to model and simulate an insulated oven with terracotta bricks. The results obtained will later allow to develop a commercial oven prototype for the grilling sector in Burkina Faso.

2. OVEN MODELING

2.1 Description of the Oven

The oven model studied is an oven which uses charcoal as fuel and consists of a casing made of iron sheet, of dimensions : L = 70 cm, W = 50 cm and H = 20 cm. For the purposes of the simulation, we consider that the thickness of the bricks varies from 0 to 7 cm.
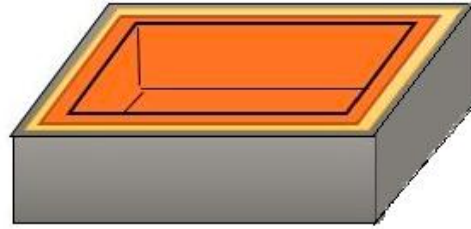

Fig. 1. Presentation of the oven model

2.2 Mathematical Formulation

2.2.1 Simplifying hypotheses

We have considered the following simplifying assumptions:

- The thermophysical properties of the materials used for oven design are almost constant,
- The ambient temperature is the same outside of the oven,
- The distribution of heat is homogeneous inside the oven,
- The properties of the air depend on the speed outside and inside they depend on the speed and the temperature.

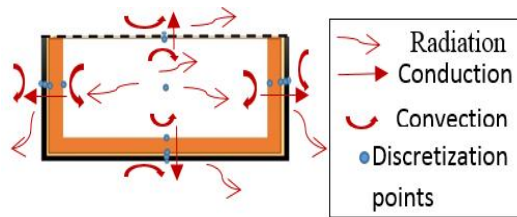Oven heat transfer model and discretization points are shown in Fig. 2.

Fig. 2. Oven heat transfer model and discretization points

2.2.2 Heat transfers equations in the oven and their discretization

Mathematical model is based on the heat balance used by others authors [22]:

At each discretization point, we have the following equation:

$$m_i c_i \frac{\partial T_i}{\partial t} = \sum_{i \neq j} g_{i,j}(T_j - T_i) + \dot{m}_{ai}^e h_a^e - \dot{m}_{ai}^s h_a^s + Q_i \quad (1)$$

Where,

m_i: Mass of node i,
C_i: Material heat capacity,
$T_{i,j}$: Temperature at nodes i and j,
$g_{i,j}$: Thermal conductance at nodes i and j,

$\dot{m}_{ai}^e$: Mass air entering in the node i,

$\dot{m}_{ai}^s$: Mass air outing the node i,

h_a^e : Enthalpy of air entering the node,

h_a^s : Enthalpy of air outing the node,

Qi: Heat source at node i

According to the heat transfer mode, the following equations are adopted:

The conductive conductance:

$$g_{i,j} = \frac{\lambda S}{e} \tag{2}$$

Where,

λ : Thermal conductivity,
S: Surface,
e : Characteristic thickness

The convective conductance:

$$g_{i,j} = h\,S \tag{3}$$

Where,

h is the convection heat transfer coefficient

The radiative conductance:

$$g_{i,j} = \varepsilon.F.\sigma(T_j + T_i)(T_j^2 + T_i^2) \tag{4}$$

Where,

ε: Emissivity of the wall,
F: Form factor,
σ: Stefan Boltzmann constant ($5,67.\,10^{-8}\mathrm{m}^{-2}\mathrm{K}^{-4}$)

The combustion chamber internal walls exchange heat by conduction, convection and radiation with the fuel, which gives the following relation:

$$m_i c_i \frac{\partial T_i}{\partial t} = g_{i,m}(T_m - T_i) + g_{i,j}(T_j - T_i) \tag{5}$$

With

$$g_{i,j} = \frac{\lambda_{i,j}.S_{i,j}}{e_{i,j}}$$

and

$$g_{i,m} = (h + h_r + \frac{\lambda_{char}}{2e_{char}})S_{i,m} \quad \text{for the side walls,}$$

$$g_{i,m} = (h + h_r + \frac{\lambda_{char}}{e_{char}})S_{i,m} \quad \text{for the bottom wall}$$

Where,

h_r : Radiative heat transfer coefficient,
λ_{char} : Thermal conductivity of charcoal,
e_{char} : Charcoal thickness

The outer walls exchange heat by convection and radiation with the external environment, which gives the following relation:

$$m_i c_i \frac{\partial T_i}{\partial t} = g_{i,j}(T_i - T_j) + g_{i,ext}(T_{ext} - T_i) + g_{i,sky}(T_{sky} - T_i) \tag{6}$$

With,

$$g_{i,ext} = (h)S_{i,ext} \quad \text{and} \quad g_{i,sky} = h_r S_{i,sky}$$

T_{sky}: Sky temperature (K),
T_{ext}: Ambient temperature (K)

The heat exchanged by the air inlets and outlets at the grid is expressed by:

$$m_i c_i \frac{\partial T_i}{\partial t} = \sum_{i \ne j} g_{i,j}(T_j - T_i) + \dot{m}_{ai}^e h_a^e - \dot{m}_{ai}^s h_a^s \tag{7}$$

The heat exchanged by the air inlets and outlets at the combustion chamber with the heat source is expressed by:

$$m_m c_m \frac{\partial T_m}{\partial t} = \sum_{m \ne j} g_{m,j}(T_j - T_m) + \dot{m}_{am}^e h_a^e - \dot{m}_{am}^s h_a^s + Q_m \tag{8}$$

The discretization of these equations gives for the external walls:

$$m_i c_i \frac{T_i^{t+\Delta t} - T_i^t}{\Delta t} = g_{i,j}(T_j^{t+\Delta t} - T_i^{t+\Delta t}) + g_{i,ext}(T_{ext} - T_i^{t+\Delta t}) + g_{i,sky}(T_{sky} - T_i^{t+\Delta t}),$$

which gives:

$$(1 + \alpha_{i,j} + \alpha_{i,ext} + \alpha_{i,sky})T_i^{t+\Delta t} - \alpha_{i,j}T_i^{t+\Delta t} = T_i^t + \alpha_{i,ext}T_{ext} + \alpha_{i,sky}T_{sky} \qquad (9)$$

With

$$\alpha_{i,j} = \frac{\Delta t * g_{i,j}}{m_i * c_i} \quad \alpha_{i,ext} = \frac{\Delta t * g_{i,ext}}{m_i * c_i}$$

and

$$\alpha_{i,sky} = \frac{\Delta t * g_{i,sky}}{m_i * c_i} \quad .$$

Δt is the step time

Likewise at the internal walls, we have:

$$(1 + \alpha_{i,j} + \alpha_{i,m})T_i^{t+\Delta t} - \alpha_{i,j}T_j^{t+\Delta t} - \alpha_{i,m}T_m^{t+\Delta t} = T_i^t \qquad (10)$$

2.3 Expressions of Heat Transfer Coefficients

The thermophysical properties of the materials used to build the oven are shown in Table 1.

2.3.1 Convective heat transfer

In the characterization of thermal transfers between any fluid and a wall, the number of Nusselt (Nu) is used. Indeed:

$$Nu = \frac{hL_c}{\lambda} \qquad (11)$$

With h the heat exchange coefficient, L_c the characteristic length and λ the thermal conductivity of the fluid.

Empirical correlations allow to determine the Nusselt number as a function of the type and the transfer regime. In our study the type of convection inside the chamber is forced convection because of the effect of the draft. The following relationship will then be used [23]:

$$Nu = 0.5(1.6 \, \mathrm{Re}^{0.5} + 2.733 \, \mathrm{Re}^{0.59}) \qquad (12)$$

Where,

$\mathrm{Re} = \dfrac{\rho \times v \times D}{\mu}$ is the Reynolds number and

$D = \dfrac{4 \times S}{P}$ the hydraulic diameter

ρ is the air density, v the kinematic viscosity of air and μ the dynamic viscosity of air

Outside the combustion chamber, we have a natural convection with the external environment. For natural convection around a vertical flat plate, Nu can be estimated by [24]:

$$Nu = 0.59(\mathrm{Pr}.Gr)^{0.025} \text{ for } 10^4 < \mathrm{Pr}.Gr < 10^9 \qquad (13)$$

and

$$Nu = 0.13(\mathrm{Pr}.Gr)^{0.33} \text{ for } \mathrm{Pr}.Gr > 10^9 \qquad (14)$$

Where,

Pr is the Prandlt number and Gr the Grashof number

The outer and inner faces of the combustion chamber exchange heat by convection with the surrounding environment. The air velocity being not negligible, we chose the Mc Adam correlation to determine the heat exchange coefficient of these faces [25].

$$h_c = 5.7 + 3.8V \qquad (15)$$

With V the air velocity

In a charcoal fireplace the correlations used for the characteristics of the air inside are [26]:

Specific heat:

$$C_p = 0.9362 + 0.0002 * T \text{ (kJ/kg.K)} \qquad (16)$$

Thermal conductivity:

$$\lambda = 0.00031847 * T^{0.7775} \text{ (W/m.K)} \qquad (17)$$

Kinematic viscosity :

$$v = (0.0000644 * T^2 + 0.0631 * T - 9.54) * 10^{-6} \text{ (m}^2\text{/s)} \qquad (18)$$

Dynamic viscosity:

$$\mu = 0{,}0447 * 10^{-5} * T^{0,7775} \text{ (kg/m.s)} \qquad (19)$$

Table 1. Thermophysical properties of materials

Materials	Heat capacity	Density	Thermal conductivity
Terracotta brick	$878 \, J.Kg^{-1}.K^{-1}$	$1800 \, Kg.m^{-3}$	$1,8 \, W.m^{-1}.K^{-1}$
Mortar	$500 \, J.Kg^{-1}.K^{-1}$	$1515 \, Kg.m^{-3}$	$1,13 \, W.m^{-1}.K^{-1}$
Iron sheet	$478 \, J.kg^{-1}.K^{-1}$	$7850 \, kg.m^{-3}$	$70 \, W.m^{-1}.K^{-1}$

Density:

$$\rho = 353/T \quad (kg/m^3) \tag{20}$$

$$\text{Pr} = 0.685 \, (\text{Constant}) \tag{21}$$

2.3.2 Radiant heat transfer

The radiative transfer coefficient between the outer wall of the oven and the celestial vault is determined by the expression [22]:

$$h_r = \frac{\sigma}{\frac{1}{\varepsilon} + \frac{1}{F_{sky}} - 1}(T_i^2 + T_{sky}^2)(T_t + T_{sky}) \tag{22}$$

In the case of a vertical wall with the celestial vault, F_{sky} is deduced by the following expression [27,28]:

$$F_{sky} = \frac{3\pi + 2b}{2\pi(3 + b)} \tag{23}$$

Where,

b is a function of the anisotropy of the sky. For an isotropic sky (b = 0), the radiative form factor corresponds to 0.5.

Among the several reported correlations to determine the temperature of the celestial vault, the one proposed by Swinbank is chosen in this work [29]:

$$T_{sky} = 0.0552 T_{ext}^{1.5} \tag{24}$$

The radiation of the charcoal is quantified by the following relation [30]:

$$F_c = \frac{(L^2 + 2(H+W)^2 - 2(H+W)\sqrt{L^2 + (H+W)^2})}{L^2} \tag{25}$$

Where,

L: Oven length,
H: Oven height,
W: Oven width

2.3.3 Energy losses calculation

The energy stored by walls is expressed by:

$$E_{st} = m_i c_i \left(\frac{T_{f-\text{int}} + T_{f-ext}}{2} - T_{ext}\right) \tag{26}$$

Where,

$T_{f-\text{int}}$: Temperature of the internal face of the material

T_{f-ext} : Temperature of the external face of the material

The energy lost by convection and radiation is expressed by:

$$E_{cv} = \sum_0^t (g_{i,ext}(T_i - T_{ext}) \times \Delta t + g_{i,sky}(T_i - T_{sky}) \times \Delta t) \tag{27}$$

The total energy lost by the oven walls is:

$$E_p = E_{st} + E_{cv} \tag{28}$$

2.4 Solving the System of Equations

At time t_0, the temperatures of the different parts of the oven are initialized at 314.15 K corresponding to the ambient temperature, then we calculate the different coefficients of heat transfer by conduction, convection and radiation. At $t_0+\Delta t$, where Δt is the step time, the resolution of the system of algebraic equations using Gauss algorithm (6-8) leads to new values of the temperature of the different parts of oven which are compared with the arbitrary values. If the difference between these two temperatures is greater than the desired precision, the values of the calculated temperatures replace the arbitrary value and the procedure described below is repeated until the convergence is obtained. The convergence was obtained when the following criterion was satisfied:

$$\frac{T^{t+\Delta t} - T^t}{T^{t+\Delta t}} \leq 10^{-3}$$

(29)

3. RESULTS AND DISCUSSION

3.1 Model Validation

The mathematical model was validated by comparing the numerical and experimental results. To perform this, an oven was built with the dimensions: L = 70 cm, W = 50 cm and H = 20 cm. The interior of the combustion chamber was then insulated with 4 cm thick terracotta bricks and assembled with a cement, sand and ash mortar. Figs. 3 and 4 show the experimental and numerical temperatures of the external walls of the oven.

Our numerical model is to describe the thermal behavior of the oven walls. Indeed, the maximum relative error $100 \times \frac{|T_{exp} - T_{num}|}{T_{exp}}$ is of the order of 13% and are due to the various empirical correlations used for the calculation of the heat transfer coefficients. T_{exp} is the experimental temperature and T_{num} the numerical temperature.

3.2 Influence of Terracotta Bricks Thickness on Heat Transfers

Figs. 4 and 5 show the influence of terracotta bricks thickness the heat transfer in the oven external walls.

The results obtained show that as soon as combustion starts in the oven, the temperature of the lateral and bottom external walls gradually increases and tends to stabilize after one hour of operation. It reaches a maximum of 400°C for the non-insulated oven (0 cm). This very high temperature is due to the high thermal conductivity of the iron sheet. In fact, heat is easily transmitted to the outside environment through the walls, which explains the huge energy losses. On the other hand, when the thickness of the insulation increases, the maximum temperature of the external walls decreases considerably. Indeed, it goes from 400°C without insulation to 90°C for a thickness of the terracotta brick of four centimeters. From four centimeters thick, the temperature curves of the exterior walls are almost confused when the thickness of the terracotta brick increases, which shows that the thickness 4 cm is the optimal thickness of thermal comfort.
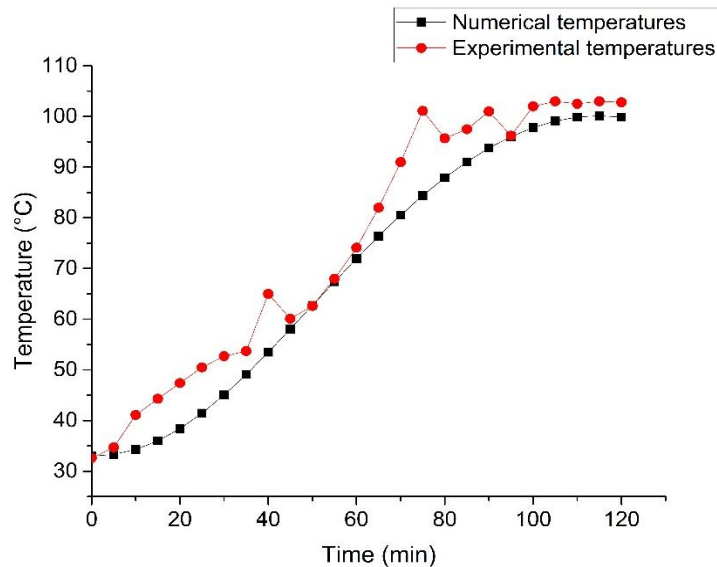

Fig. 3(a). Model validation for bottom wall (Charcoal mass: 3 Kg, terracotta bricks thickness: 4 cm, terracotta bricks thermal conductivity: 1.18 $W.m^{-1}.K^{-1}$, terracotta bricks density: 1800 $Kg.m^{-3}$, terracotta bricks heat capacity: 878 $J.Kg^{-1}.K^{-1}$, Mortar thickness: 0.5 cm, Mortar conductivity: 1.2 $W.m^{-1}.K^{-1}$, Mortar density 1515 $Kg.m^{-3}$, Mortar heat capacity: 800 $J.Kg^{-1}.K^{-1}$, iron sheet thickness: 0.15 cm, Iron sheet thermal conductivity: 70 $W.m^{-1}.K^{-1}$, Iron sheet density: 7850 $Kg.m^{-3}$, Iron sheet heat capacity: 478 $J.kg^{-1}.K^{-1}$)
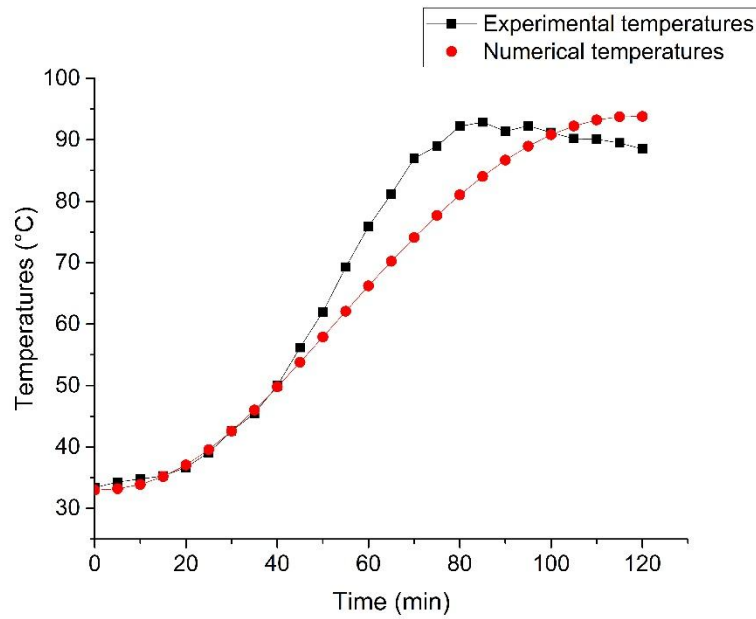
Fig. 3(b). Model validation for lateral walls (Charcoal mass: 3 Kg, terracotta bricks thickness: 4 cm, terracotta bricks thermal conductivity: 1.18 $W.m^{-1}.K^{-1}$, terracotta bricks density: 1800 $Kg.m^{-3}$, terracotta bricks heat capacity: 878 $J.Kg^{-1}.K^{-1}$, Mortar thickness: 0.5cm, Mortar conductivity:1.2 $W.m^{-1}.K^{-1}$, Mortar density: 1515 $Kg.m^{-3}$, Mortar heat capacity: 800 $J.Kg^{-1}.K^{-1}$, iron sheet thickness: 0.15 cm, Iron sheet thermal conductivity: 70 $W.m^{-1}.K^{-1}$, Iron sheet density : 7850 $Kg.m^{-3}$, Iron sheet heat capacity : 478 $J.kg^{-1}.K^{-1}$)
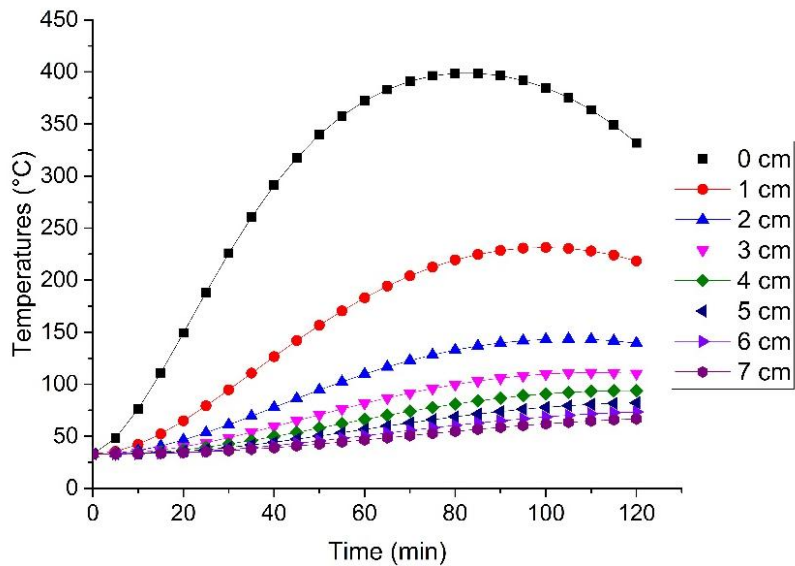
Fig. 4. Lateral walls external temperature profiles for thicknesses of terracotta brick from 0 to 7 cm
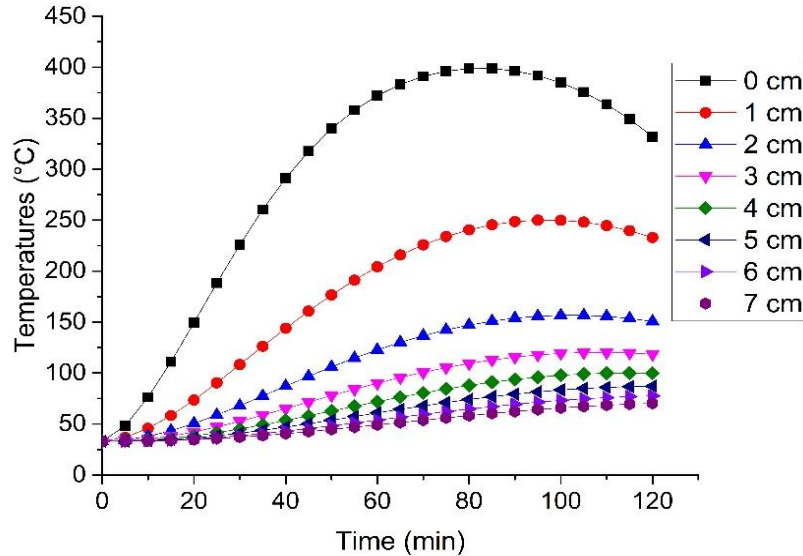
Fig. 5. Bottom walls external temperature profiles for thicknesses of terracotta bricks from 0 to 7 cm

3.3 Influence of Terracotta Bricks Thickness on the Energy Losses by Oven Walls

Figs. 6, 7 and 8 show the influence of terracotta bricks thickness on the energy losses by oven walls.

It is noted that the heat losses by convection and radiation decrease with the increase in the thickness of the bricks. In fact, when the thickness of the bricks increases, the temperature of the external walls drops as observed in Figs. 4 and 5.

It can be seen that the storage losses increase with the increase in the thickness of the bricks. Indeed, when the thickness of the bricks increases, their mass increases, which increases the energy storage.

The total energy lost by the walls as a function of the thickness of the bricks is shown in Fig. 8.

We note that when the thickness of the terracotta brick increases, the total amount of energy lost by the walls decreases to a brick thickness of 3 cm, then increases again with the thickness of the bricks. So, with three centimeters of thickness, we have the minimum energy loss through the walls. The thickness of 3 cm is the optimal thickness to minimize energy loss through the walls compared to the uninsulated oven.

3.4 Influence of Terracotta Bricks Thickness on the Energy Savings by the Insulated Oven

Fig. 9 shows the influence of terracotta bricks thickness on the energy savings performed by insulation.

The result obtained is an accordance with the result related to energy losses (Fig. 8). Indeed, the maximum energy saving (70%) is achieved at the thickness 3 cm, which also represents the thickness where the losses are minimal. For the thermal comfort thickness (4 cm), the energy saving is around 68%.

3.5 Influence of Terracotta Bricks Thickness on the Energy Efficiency of the Insulated Oven

Fig. 10 show the influence of terracotta bricks thickness on the energy efficiency of the insulated oven.

We can see that without insulation (0 cm), the efficiency of the oven is around 15-17%, which corresponds to the efficiency of first generation ovens as mentioned in the literature [31]. As for the previous results, the maximum efficiency (25-29%) is obtained for a brick thickness of 3 cm. For the thickness of thermal comfort, the maximum efficiency is between 24 and 28%.
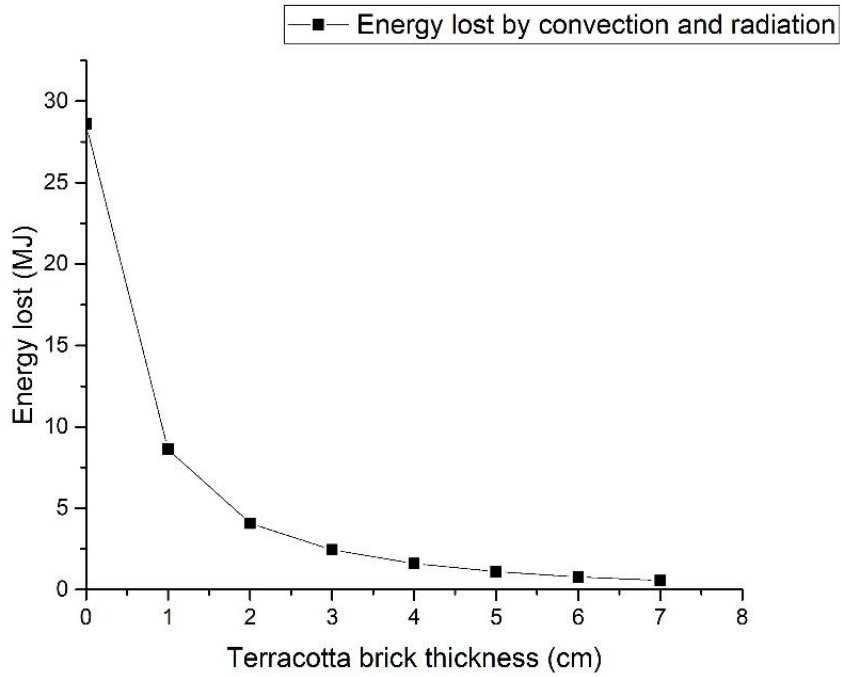
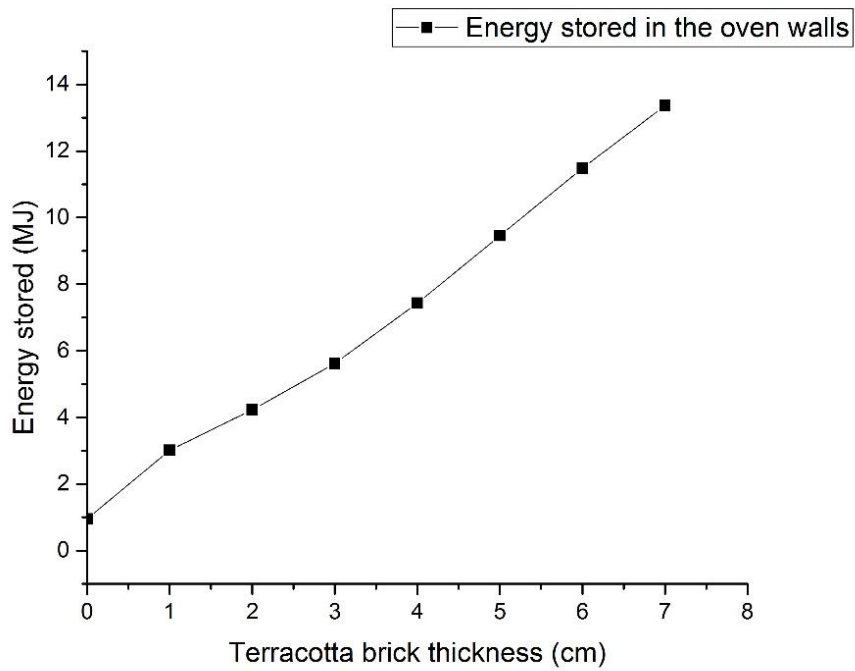**Fig. 6. Energy lost by convection and radiation with the ambient**

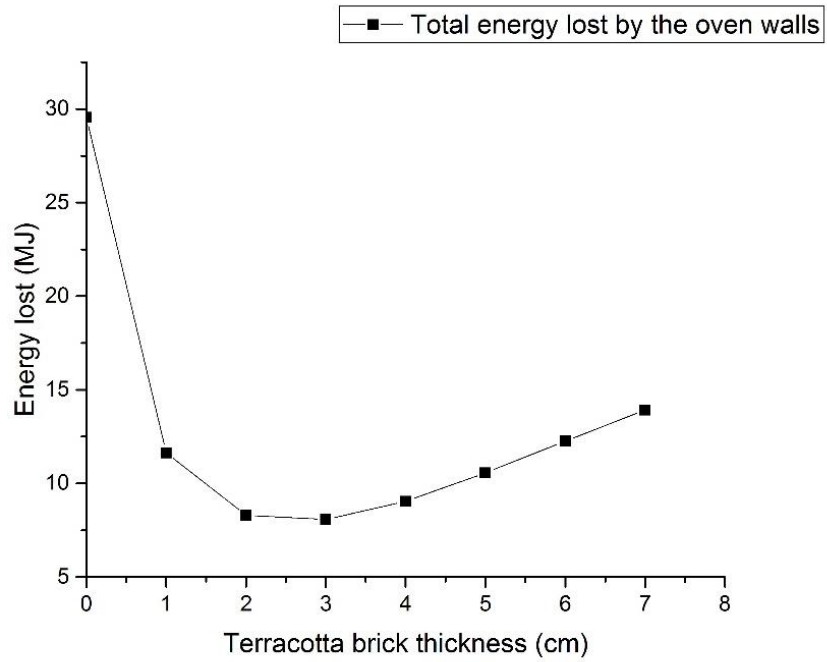**Fig. 7. Energy stored in the oven walls**

Fig. 8. Total energy lost by oven walls with terracotta brick thicknesses from 0 to 7 cm
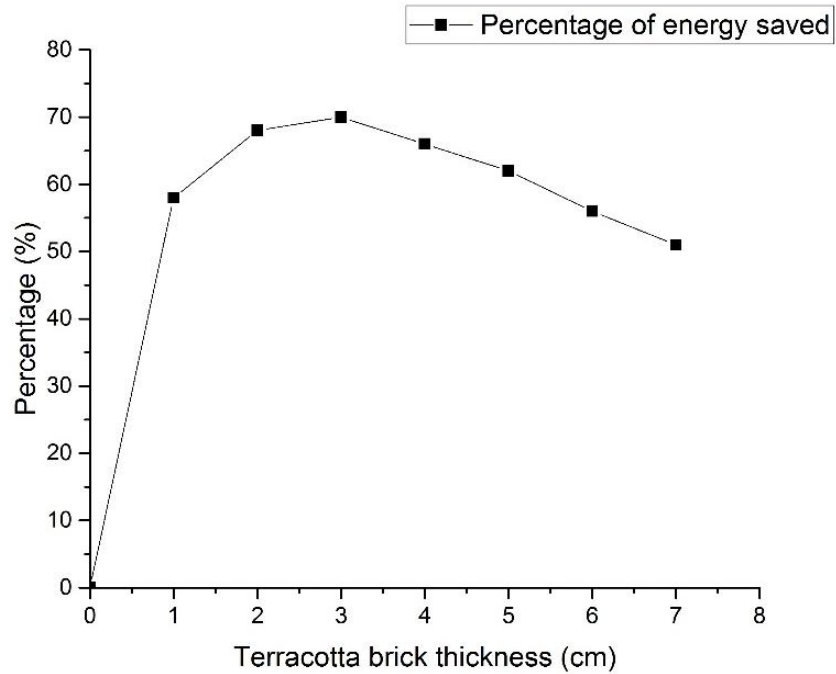

Fig. 9. Percentage of energy saved with terracotta brick thicknesses from 0 to 7 cm
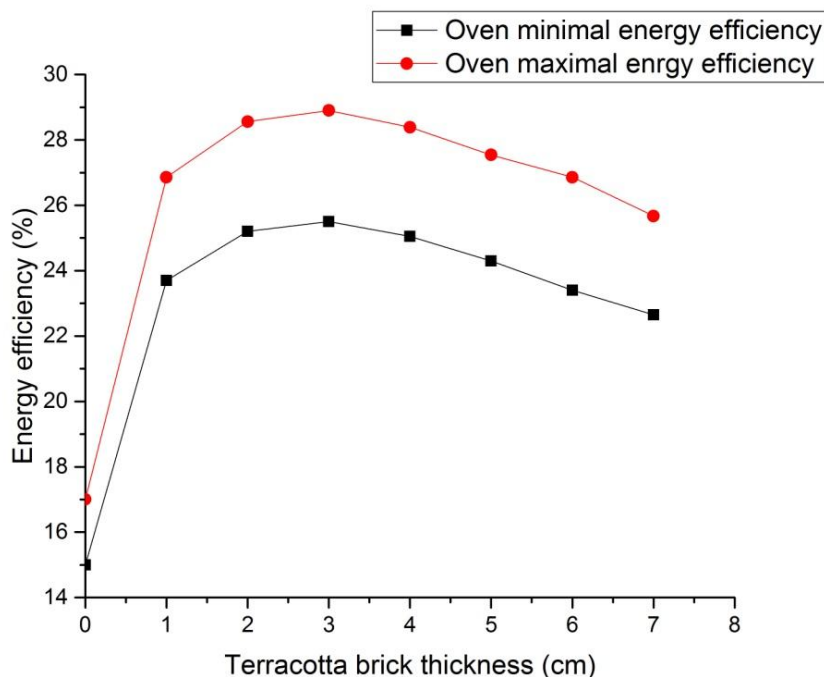
Fig. 10. Influence of the thickness of terracotta bricks on the oven energy efficiency

4. CONCLUSION

In this work, the performances achieved by an insulated oven with terracotta bricks compared to an uninsulated oven were highlighted by a numerical study. The numerical methodology is based on the nodal method and the transfer equations obtained by making an energy balance on each node have been discretized using an implicit scheme with finite differences and resolved by the Gauss algorithm. The main results are summarized as follows:

- The insulation of the oven with terracotta bricks significantly reduces heat loss through the walls. However, the level of loss reduction depends on the thickness of the brick.
- The optimal thickness of the bricks for energy savings is 3 cm while the optimal thickness for thermal comfort is 4 cm.
- The energy savings achieved for optimal thicknesses are between 60 and 70%.
- The maximum efficiency (25-29%) is obtained for a brick thickness of 3 cm. For the thickness of thermal comfort, the maximum efficiency is between 24 and 28%.

These results show that terracotta bricks can be used to reduce the energy consumption caused by grilling equipment.

ACKNOWLEDGEMENTS

COMPETING INTERESTS

Authors have declared that no competing interests exist.

REFERENCES

1. Sakiru AS, Usama AM, Gerald GGG, Muhammad S. The impact of biomass energy consumption on pollution: Evidence from 80 developed and developing countries. Environmental Science and Pollution Research. 2018;25:22641–22657. DOI:https://doi.org/10.1007/s11356-018-2392-5

2. Keles S, Bilgen S, Kaygusuz K. Biomass energy source in developing countries.

Journal of Engineering Research and Applied Science. 2017;6(1):566-576.

3. Melike B, Fulya Ö. Woody biomass energy consumption and economic growth in Sub-Saharan Africa, Istanbul Conference of Economics and Finance, ICEF. Istanbul, Turkey. Procedia Economics and Finance. 2015;38:287–293.
    DOI:https://doi.org/10.1016/S2212-5671(16)30202-7

4. Matthew FC, Caradee YW, Francois V, Helem R, Fiona S, Barend E. Impacts of climate change on health and wellbeing in South Africa. International Journal of Environmental Research and Public Health. 2018;15(9):2-14.
    DOI:https://doi.org/10.3390/ijerph15091884

5. Pyhälä A, Fernandez-Llamazares A, Lehvävirta H, Byg A, Ruiz-Mallén I, Salpeteur M, Thornton TF. Global environmental change: Local perceptions, understandings and explanations. Ecology and Society. 2016;21(3):25.
    DOI:https://doi.org/10.5751/ES-08482-210325

6. Stephane H, Marianne F, Edward BB. Poverty and climate change: Introduction. Environment and Development Economics. 2018;23(3):217-233.
    DOI:https://doi.org/10.1017/S1355770X18000141

7. Butt EW, Rap A, Schmidt A, Scott CE, Pringle KJ, Reddington CL, et al. The impact of residential combustion emissions on atmospheric aerosol, human health, and climate. Atmos. Chem. Phys. 2016;16: 873–905.
    DOI:https://doi.org/10.5194/acp-16-873-2016

8. Smith KR, Samet JM, Romieu I, Bruce N. Indoor air pollution in developing countries and acute lower respiratory infections in children. Thorax. 2000;55: 518–532.
    DOI:https://doi.org/10.1136/thorax.55.6.518

9. Charles WS. Black carbon: The dark horse of climate change drivers. Environ Health Perspect. 2011;119(4):A172–A175.

10. Ram PK, Alok P, Krishan K. A review on the atmospheric Non Methane Hydrocarbons (NMHCs) study in India. Current World Environment. 2017;12(2): 278-287.

11. World Health Organization. World Health Statistics 2018: Monitoring health for the SDGs, sustainable development goals. WHO; Geneva, Switzerland; 2018.

12. MacCarty N, Ogle D, Still D, Bond T, Roden C. A laboratory comparison of the global warming impact of five major types of biomass cooking stoves. Energy Sustain Dev. 2008;12(2):56–65.
    DOI:https://doi.org/10.1016/S0973-0826(08)60429-9

13. Anthony AB, Gilbert N, Sarah K, Yonah KT. Design of an improved cooking stove using high density heated rocks and heat retaining techniques. Journal of Renewable Energy. 2018;18:1-9.
    DOI: https://doi.org/10.1155/2018/9620103

14. Kuhe A, Iortyer HA, Iortsor A. Performance of clay wood cook stove: An analysis of cost and fuel savings. Journal of Technology Innovations in Renewable Energy. 2014;3:94-98.
    DOI:https://doi.org/10.6000/1929-6002-2014.03.03.2

15. Komi AA, Koffi S, Kokou N, Tchamou S, Kossi N. Study and design of an improved clay conical stove. International Journal of Recent Scientific Research. 2018;9(12): 29909-29915.
    DOI:https://dx.doi.org/10.24327/ijrsr.2018.0912.2958

16. Abanda FH, Manjia MB, Cole E, Mempouo B. The potential of efficient improved mud-brick cookstove in Cameroon: An exploratory study. Environmental Management and Sustainable Development. 2015;4(1):106-119.
    DOI:https://doi.org/10.5296/emsd.v4i1.6715

17. Sawadogo GL, Igo SW, Compaoré A, Ouedraogo D, Chesneau X, Zeghmati B. Experimental and numerical study of energy losses in a barbecue oven in Burkina Faso. Open Journal of Energy Efficiency. 2020;9(1):31-52.
    DOI:https://doi.org/10.4236/ojee.2020.91003

18. Amkpa JA, Nur AB. Thermal conductivity of Aloji fireclay as refractory material. International Journal of Integrated Engineering. 2016;8(3):16-20.
    DOI:https://doi.org/10.5296/emsd.v4i1.6715

19. Olasupo OA, Borode JO. Development of insulating refractory ramming mass from some Nigerian refractory raw materials. Journal of Minerals & Materials Characterization & Engineering. 2009;8(9): 667-678.

DOI:https://doi.org/10.4236/jmmce.2009.89058

20. Aurélie MICHOT. Caractéristiques thermophysiques de matériaux à base d'argile: Evolution avec des traitements thermiques jusqu'à 1400°C. Thèse de Doctorat, Université de LIMOGES; 2008.

21. Pierre MEUKAM. Valorisation des briques de terre stabilisées en vue de l'isolation thermique des bâtiments. Thèse de doctorat de 3ème cycle, en co-tutelle entre l'Université de Cergy Pontoise et l'Université de Yaoundé I; 2004.

22. Compaore A. Etude des performances thermiques d'un habitat type du Burkina Faso. Application: Contribution à la mise en place d'une règlementation thermique. Thèse de doctorat de l'Université Ouaga I Pr Joseph KI ZERBO; 2018.

23. McCarty NA, Bryden KM. A generalized heat-transfer model for shielded-fire. Energy for Subtainable Development. 2016;33:96-107. DOI:https://doi.org/10.1016/j.esd.2016.03.003

24. Eyglunent B. Manuel de thermique-Théorie et pratique, Hermès- Lavoisier; 2003.

25. Adams M. Transmission de la chaleur, Dunod. Paris; 1964.

26. Kshirsagar MP, Kalamkar VR. A mathematical tool for predicting thermal performance of natural draft biomass cookstoves and identification of a new operational parameter. Energy. 2015;93: 188-201. DOI:https://doi.org/10.1016/j.energy.2015.09.015

27. Ivanova SM. Estimation of background diffuse irradiance on orthogonal surfaces under partially obstructed anisotropic sky Part I – Vertical surfaces. Solar Energy. 2013;95:376–391. DOI:https://doi.org/10.1016/j.solener.2013.01.021

28. Ramírez-Faz J, Casares FJ, Lopez-Luque R. Development of synthetic hemispheric projections suitable for assessing the sky view factor on vertical planes. Renewable Energy. 2015;74:279-286. DOI:https://doi.org/10.1016/j.renene.2014.08.025

29. Boubghal SOA. Etude paramétrique d'un capteur solaire plan à air destiné séchage. Revue des Energies Renouvelables SMSTS'08 Alger. 2008;255–26.

30. Khummongkol P, Wibulswas P, Bhaitacharya SC. Modeling of a charcoal cook stove. Energy. 1988;13:813-821. DOI:https://doi.org/10.1016/0360-5442(88)90086-2

31. Global Alliance for Clean Cookstoves. Handbook for biomass cookstove research, design and development: A practical guide to implementing recent advances. Massachusetts Institute of Technology D-lab; 2017.

Peer-review history:
The peer review history for this paper can be accessed here:
http://www.sdiarticle4.com/review-history/58314